REVIEW ON NUCLEON STRUCTURE FUNCTIONS

JOEL FELTESSE
CEA, DAPNIA/DSM/Service de Physique des particules, CE-Saclay
F-91191 Gif-sur- Yvette Cedex, France
E-mail: Feltesse@hep.saclay.cea.fr

ABSTRACT

The 1994 preliminary data of the HERA experiments H1 and ZEUS on the proton structure function are presented together with the final data of the muon fixed target experiments E665 at FNAL and NMC at CERN. Perturbative QCD interpretations and extraction of α_s at low x are discussed,

1. Introduction

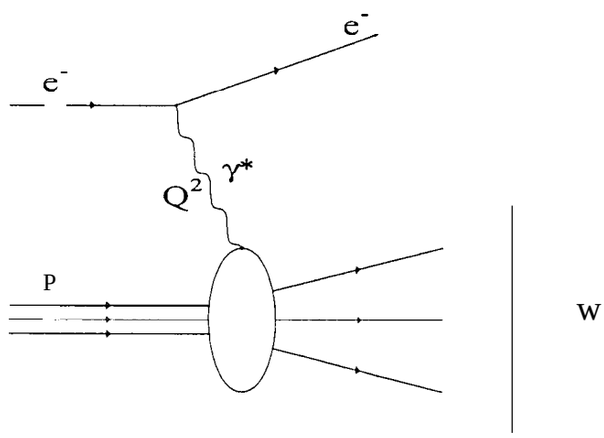

Fig. 1. Basic Feynman diagram for electron proton deep inelastic scattering. Q^2 is minus the squared four momentum transferred or minus the squared mass of the virtual photon, W is the virtual photon-proton centre of mass energy.

In lepton-nucleon scattering the lepton probes the structure of the nucleon with a spatial resolution $\lambda \sim \frac{\hbar c}{\sqrt{Q^2}}$ where Q^2 is minus the squared four-momentum of the exchanged virtual photon (Fig. 1), At HERA Q^2 can reach 90000 GeV^2 and λ can be as low as $\sim$ 0.001 fm, i.e. 1000 times smaller than the size of the proton. In the case of an elastic collision W, the outgoing invariant hadronic mass (Fig, 1), is equal to M the mass of the nucleon and ν the energy lost by the lepton in the nucleon frame is simply

$$\nu = \frac{Q^2}{2M} \tag{1}$$

In other words, using the Bjorken variable $x = \frac{Q^2}{2M\nu}$ the elastic cross section should have a peak around x = 1. Similarly when the lepton scatters elastically off valence

quarks of the nucleon, the cross section should have a peak around $x = \frac{1}{3}$ and go to zero when x goes to zero.
More precisely, the inclusive differential cross section for DIS of a charged lepton off a nucleon is given in terms of structure functions as :

$$\frac{d^2\sigma(l^{\pm}N)}{dx dQ^2} = \frac{2\pi\alpha^2}{Q^4 x}\left[\left(2\,(1-y) + \frac{y^2}{1+R}\right)F_2(x,Q^2) \mp \left(2y - \frac{y^2}{2}\right)xF_3(x,Q^2)\right] \quad (2)$$

with

$$R = \frac{F_2 - 2xF_1}{2xF_1} = \frac{F_L}{2xF_1} \quad (3)$$

where F_L is the longitudinal structure function. The contribution from F_L is negligible except at large y, where y is the fractional energy transferred to the photon in the nucleon centre of mass. In the highest Q' range accessed by the present data ($Q^2 \approx$ 5000 GeV^2) the contribution of the structure function xF_3 is still a small correction. In the Quark Parton Model, the structure function F_2 is simply related to $q_i(x)$ the probability of finding the quark i in the nucleon carrying a fraction x of the proton momentum :

$$F_2(x) = \sum_i e_i^2\, x(q_i(x) + \bar{q}_i(x)) \quad (4)$$

where e_i is the electric charge of the quark i.

In the naive approach of quark constituents in the nucleon, the structure function is expected to have a peak around x = $\frac{1}{3}$ and to go to zero when x goes to zero or to one. This naive approach of the x dependence has been well supported by the lepton-nucleon data on fixed targets accumulated at SLAC, Fermilab and CERN up to the late eighties. In 1992, the data from the electron-proton collider HERA has completely ruled out this approach and demonstrated a dramatic rise of the structure function when x goes to zero [a].

In this review, some of the salient predictions of QCD on the x and Q^2 dependence of the structure function are reminded. Then, the most recent data on fixed target and in collider mode are presented, Finally, the perturbative QCD interpretation of the data is discussed.

2. Theoretical Expectations

Although the full x and Q^2 dependence of the structure functions is not given by perturbative QCD (PQCD), there are many prescriptions which can be compared to the data :

. Q^2 evolution

[a] The rise could have been anticipated from the latest results of the NMC collaboration at CERN

- x evolution of the gluon density at very low x
- asymptotic behaviour when $x \to$ O
- behaviour for x close to x = 1
- $F_L(x, Q^2)$
- Non Singlet and Singlet Sum Rules

2.1. Q^2 evolution

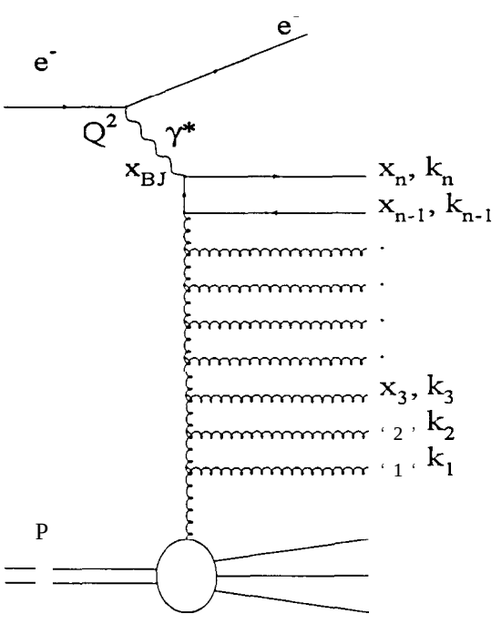

Fig. 2. Diagrammatic representation of the gluon rungs contributing to deep inelastic scattering.

[redacted]

the summation, gluons have ordered longitudinal momenta (momentum conservation) but also strongly ordered transverse momenta

$$x \leq x_n \leq \ldots \leq x_2 \leq x_1$$
$$Q^2 \gg k_n^2 \gg \cdots \gg k_2^2 \gg k_1^2 \gg Q_0^2 \tag{5}$$

The summation can be used in simulation programs to provide prediction on the hadronic final states and provides the so-called Dokshitzer Gribov Lipatov Altarelli Parisi (DGLAP) differential equations on Q^2 evolution of structure functions [3].

In Leading Order (LO), for Non-Singlet [b] structure functions $F^{NS}(x,Q^2)$, the Q^2 derivative at fixed x depends only on the quark densities at momentum fractions above x, but for Singlet [c] structure functions $F^S(x,Q^2)$, the Q^2 derivative depends on both the quark and the gluon densities :

$$\frac{\partial F^{NS}(x,Q^2)}{\partial \log(Q^2)} = \frac{\alpha_s(Q^2)}{2\pi}\int_x^1 \frac{dy}{y} \quad F^{NS}(y,Q^2)P_{qq}^{NS}(\frac{x}{y}) \tag{6}$$

$$\frac{\partial F^S(x,Q^2)}{\partial \log(Q^2)} = \frac{\alpha_s(Q^2)}{2\pi}\int_x^1 \frac{dy}{y} \quad \left[F^S(y,Q^2)P_{qq}^S(\frac{x}{y}) + 2n_f g(y,Q^2)P_{qg}^S(\frac{x}{y})\right] \tag{7}$$

$$\frac{\partial g(x,Q^2)}{\partial \log(Q^2)} = \frac{\alpha_s(Q^2)}{2\pi}\int_x^1 \frac{dy}{y} \quad \left[F^S(y,Q^2)P_{gq}^S(\frac{x}{y}) + g(y,Q^2)P_{gg}^S(\frac{x}{y})\right] \tag{8}$$

where the P_{qq}, P_{gq} and P_{gg} are known splitting functions, n_f is the number of flavours and $xg(x,Q^2)$ is the gluon distribution. In parton language, the equations predict that when Q^2 increases there are more partons at low x ($x < 0.1$) and less partons at large x ($x > 0.2$).

The differential equations arise from the resummation of a series of $(\alpha_s \log(Q^2/Q_0^2))^n$ which is a priori only valid in the kinematical domain of the Leading Log Approximation (LLA(Q^2)) defined by (see Fig.3) :

$$\begin{aligned} \alpha_s(Q^2)\log(Q^2/Q_0^2) &\sim 1 \\ \alpha_s(Q^2)\log(1/x) &<<1 \\ \alpha_s(Q^2) &<<1 \end{aligned} \tag{9}$$

The validity of the DGLAP differential equations has been very precisely checked in fixed target experiments and provided one of the best determinations of α_s 4 Before data from HERA have become available at very low x it has been commonly guessed that these equations would only be valid at about x >10-2 and Q^2 >4 GeV^2.

2.2. x evolution

At very low x the so-called Balitski Fadin

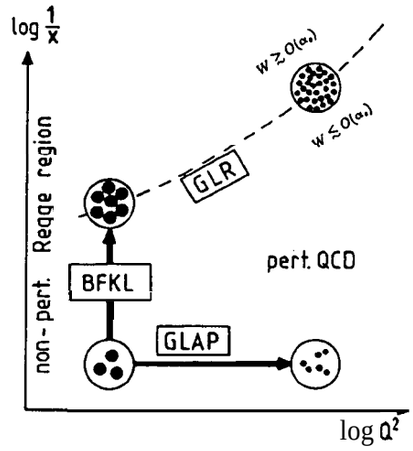

Figure 3: Schematic evolution of the quark densities in various (x, Q^2) regions according to the dominant dynamical effects. The dashed line is the theoretical limit of validity of perturbative QCD. Picture borrowed to reference [10].

The differential equation is based on summation of $(\alpha_s$

$$f(x, k^2) = \frac{\partial x g(x, Q^2)}{\partial \log(Q^2)}|_{Q^2=k^2} \tag{12}$$

The kernel $K(k, k')$ is a known function 5. Q_0 is an energy cut-off to prevent divergence of the kernel at $Q^2 = 0$. When x decreases, the equation evolution predicts a steep rise of the gluon density.

As in DGLAP evolution, the evolution at small x can be described as a branching process in the initial state, but with different orderings [6,7,8]. In the parton chain there is no strong ordering in k_n^2 but a strong ordering in x_n

$$\begin{gathered} x \ll x_n \ll \cdots \ll x_2 \ll x_1 \\ Q^2 \geq k_n^2 \geq \cdots \geq k_2^2 \geq k_1^2 \geq Q_0^2 \end{gathered} \tag{13}$$

The phase space available is larger than for strong transverse momentum ordering. There is “diffusion” or “random walk” in transverse momentum along the gluon chain. The difference of level of ordering in the gluon emission between DGLAP mechanism

(strong order) and BFKL mechanism (soft order) has been exploited to look for signatures of the BFKL mechanism 9.

2.3. *Asymptotic behaviour when $x \to O$.*

A long time ago, in 1974, it has been demonstrated that non-Abelian gauge theories are asymptotically free [11]. This is the fundamental property of QCD. A surprising consequence [12] of the asymptotic freedom is that, on the basis of certain uniformity assumptions, the structure function F_2 of the nucleon should grow faster than any power of $\log \frac{1}{x}$ and slower than any power of $\frac{1}{x}$ as $x \to$ O. This crucial property of QCD was forgotten for many years.

More recently [13] it has been shown that perturbative QCD predicts that the structure function F_2 should exhibit asymptotic scaling in the two variables $\sqrt{(\log 1/x)(\log\log Q^2)}$ and $\sqrt{(\log 1/x)/(\log\log Q^2)}$ at sufficiently large Q^2 and low x values. The double scaling behaviour is derived provided that the small x behaviour of the input distribution is sufficiently soft at some rather low Q^2 value ($Q_0^2 \sim 1.\ \mathrm{GeV}^2$). The growth of F_2 at small x is due to the collinear singularity in the triple gluon vertex, it is thus directly related to the actual value of α_s. In the asymptotic region free of non-perturbative uncertainties and where the data agree with the double scaling prediction, the growth of F_2 can be used to provide a precise determination of α_s (see section 4.4).

A different approach at low x is to resum the (α_s log l/z)" terms as accomplished by the BFKL equation. When the effect of the running coupling constant is neglected, i.e. in a small range of Q^2, the BFKL evolution equation of the gluon can be solved analytically. The solution exhibits a Regge type $x^{-\lambda}$ dependence with

$$\lambda = \frac{12\alpha_s}{\pi} \log 2 \approx 0.5 \tag{14}$$

The quantity $1 + \lambda$ is equal to the intercept of the so called BFKL bare pomeron which is very different from the 1.08 intercept of the effective soft pomeron which describes so well the energy dependence of all hadron-hadron and photon-hadron cross sections [14]. When the running of α_s and the strict conservation of energy is taken into account the exponent λ is expected to be a bit smaller [15,16,17].

For completeness we should also mention that the rise of the gluon density has to be damped at some sufficiently small value of x by saturation (shadowing) effects when the parton density is so large that the partons can no longer be considered as independent. The Gribov Levin Ryskin (GLR) equation [18] is the first attempt to describe the shadowing correction. It is a perturbative QCD calculation applied in the transition region to the unknown domain of non-perturbative QCD (see Fig.3). Shadowing effects are however expected to be relatively weak in the HERA kinematical

domain [19,17,20].

2.4. Behaviour near $x = 1$,

Assuming that the structure functions behave as

$$F_2(x, Q^2) \sim A(Q^2)(1-x)^{\nu(Q^2)} \tag{15}$$

for x close to x = 1, the following counting rule has been obtained at leading order in α_s [21]

$$\nu_V = \nu_0 - \frac{16}{33-2n_f}\log(\alpha_s(Q^2)) \tag{16}$$

$$\nu_G = \nu_V + 1 \tag{17}$$

$$\nu_{sea} = \nu_V + 2 \tag{18}$$

where the suffixes *V, G* and sea are refering to the valence, gluon and sea distributions and n_f is the number of flavors. ν_o is not given by the theory, although one expects 22 $\nu_0 \sim 2$ *to 3,* These countin$_g$ rules have not yet been precisely checked in the data due to the very small rates at large x.

2.5. $F_L(x, Q^2)$

In the naive parton model and in leading order of QCD the longitudinal structure function F_L is zero, In next-to-leading order of PQCD F_L gets contributions in α_s from both quarks and gluons :

$$F_L(x, Q^2) = \frac{\alpha_s(Q^2)}{2\pi}x^2\int_x^1 \frac{dy}{y^3}\left[\frac{8}{3}F_2(y, Q^2) + 2\sum_{i=1}^{2n_f} e_i^2(y-x)g(y, Q^2)\right]. \tag{19}$$

F_L should vanish smoothly at large Q^2 as $\alpha_s(Q^2)$ and get sizeable contributions at low x (x < 0.1) due to the increase of the sea and of the gluon distributions. There are no measurements so far at x <0.1, In the HERA domain, to extract the structure function F_2 from the cross section (equation 2) assumptions based on the perturbative QCD expression (equation 19) are made.

2.6. Sum Rules

The moments of structure functions are defined as

$$M_n(Q^2) = 11\ x^{n-2}F(x, Q^2)dx\ . \tag{20}$$

It can be demonstrated in QCD that at leading order, moments order one (resp. two) are Q^2 independent for Non-Singlet (resp. Singlet) structure functions [1,2] :

$$\int_0^1 \frac{dx}{x} F_{NS}(x, Q^2) = J_0^{NS} + J_1^{NS} \frac{\alpha_s(Q^2)}{4\pi} + ... \tag{21}$$

$$\int_0^1 dx F_S(x, Q^2) = J_0^S + J_1^S \frac{\alpha_s(Q^2)}{4\pi} + ... \tag{22}$$

Two usual Non-Singlet Sum Rules are given below :

. Gross Llewellyn-Smith Sum Rule 23 :

in neutrino-nucleon scattering

$$\int_0^1 \frac{dx}{x} x F_3^{\nu}(x, Q^2) = 3(1 - \frac{\alpha_s(Q^2)}{2\pi} + ...) \tag{23}$$

QCD corrections are known up to α_s^3 terms [24]. It is one of the best ways to extract α_s from neutrino scattering experiment (see section 3.3)

• Gottfried Sum Rule 25 :

$$\int_0^1 \frac{dx}{x} (F_2^{ep} - F_2^{en}) = \frac{1}{3} + \frac{2}{3} \int_0^1 dx(\bar{u} - \bar{d}) + k_0 \frac{\alpha_s(Q^2)}{\pi} \tag{24}$$

where k_0 is a known minute constant [26].

The sum rule of the singlet function F_2^S is usually called the momentum sum rule. The asymptotic value is not given by the quark parton model but by QCD :

$$lim_{Q^2 \to \infty} \int_0^1 F_2^S(x, Q^2) dx = \frac{3n_f}{2n_g + 3n_f} < e_q^2 > = \frac{5}{42} \tag{25}$$

where $< e_q^2 >$ is the average square quark charge on the n_f flavors. There is however no absolute prediction at finite Q^2.

3. The New Data

New results on the proton structure function

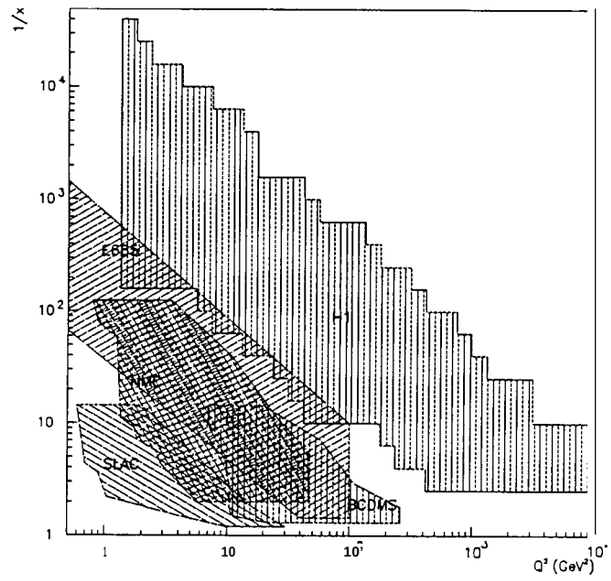

Fig. 4.

The NMC collaboration at CERN has published [27] the final analysis of the muon

$0.004 < x < 0.15$ and extrapolated to $x = 0$. The fit yields the values $a = 0.20 \pm 0.03$

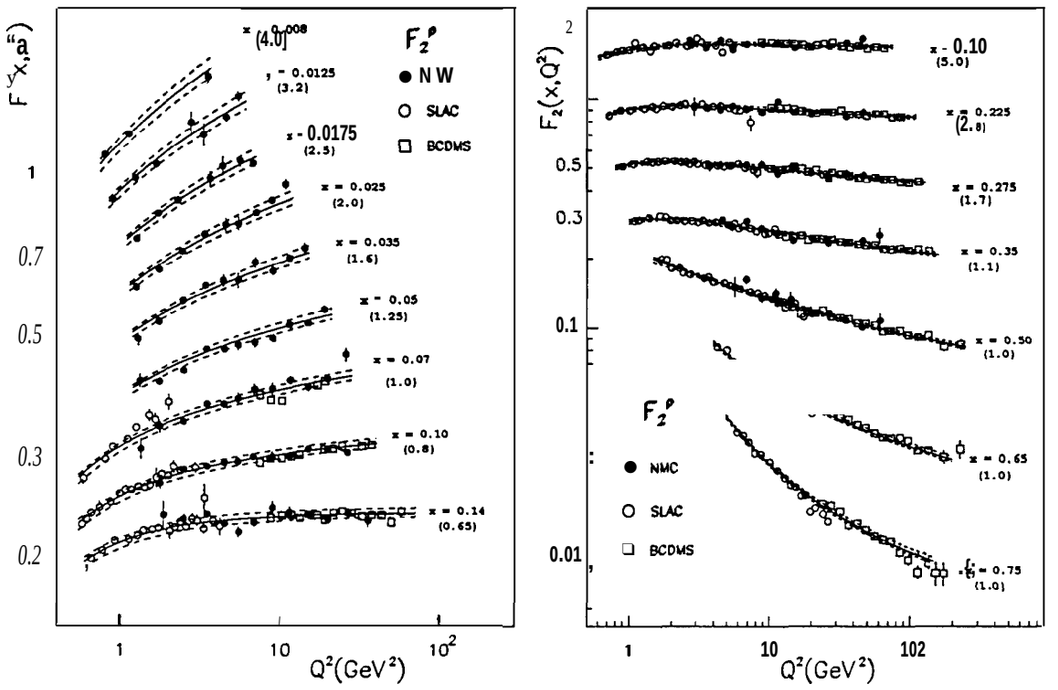

Fig. 5. The proton structure function F_2^p. The NMC results are compared with those of SLAC and BCDMS. The SLAC and BCDMS values were rebinned to NMC x bins. The data sets have been renormalised according to the values resulting from the common fit. BCDMS data have also been adjusted for the energy calibration obtained from the fit. The solid curve is the result of the common fit to the three data sets. The error bars are represent the statistical errors. The dashed curves indicate the total uncertainty,

and b = 0,59 $\pm$ 0.06 and a contribution to S_G of 0.013 $\pm$ 0.005 (stat) for x < 0.004. The result is close to the previous published value S_G = 0.240 $\pm$ 0.01637. The data were not corrected for shadowing effects in deuterium, but if anything they should even reduce S_G by 1570.

The NMC result is significantly below the simple quark parton model value of 1/3 (equation 24). The light-quark sea in the nucleon is flavour asymmetric. There are more $\bar{d}$ than ii in the proton, This interpretation has however been questioned because the extrapolation to x = O is model dependent. It is possible, although a bit artificial, to build parametrizations of the valence quarks momentum distributions which describe the NMC data and yet satisfy the Gottfried sum rule [38].

3.2. *E665*

This year, the final data of the E665 collaboration at the Tevatron at FNAL on the proton structure function $F_2(x,Q^2)$ have been presented 28 . The data were

taken in 1991 in the 400-550 GeV muon beam at FNAL. The integrated luminosity on a hydrogen target is 0.7 pb^{-1}. The kinematic range starts at Q^2 = 0.1 GeV^2 and x = 8 10^{-4}. The data are discussed in detail in another contribution to this workshop [39]. The x behaviour of F_2 and the comparison with NMC data will be discussed below together with the HERA data.

3.3. *CCFR*

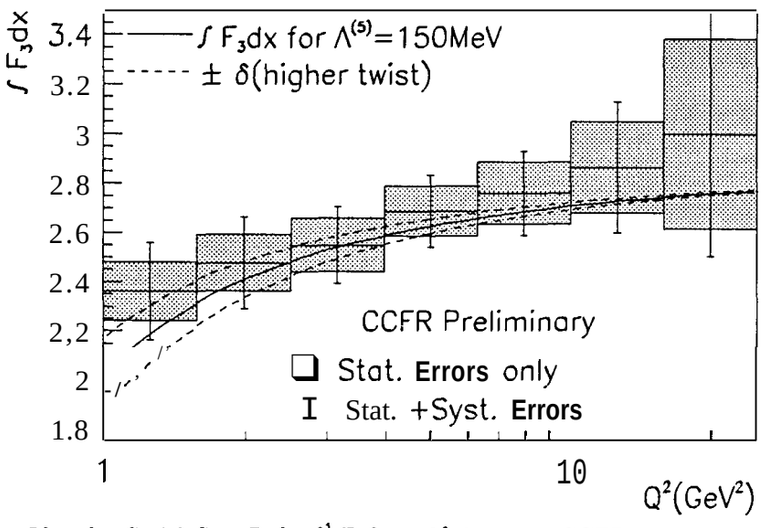

Fig. 6. The Gross Llewelyn Smith Sum Rule. $\int_0^1 F_3 dx$ vs Q^2 from the CCFR Collaboration together with the theoretical prediction for $\Lambda^{(5)}_{\overline{MS}}$=150MeV. The dashed lines represent the uncertainty in the higher twist corrections.

There are no new data from the neutrino scattering experiment CCFR at FNAL but a new evaluation of the Gross Llewelyn Smith Sum Rule, The goal is to determine $\alpha_s(Q^2)$ from the equation 23. The challenge in evaluating $\int_0^1 F_3 dx$ is that for a given Q^2 value, there is a limited x region that is accessible by any one experiment. one way to evaluate $\int_0^1 F_3 dx$ over all x is to extrapolate xF_3 from the measured Q^2 region to an average Q_0^2 value. A previous CCFR analysis 40 found that for Q_0^2 = 3 GeV^2,

$$\int_0^1 F_3 dx = 2.50 + \ 0.018 + \ 0.078 \tag{27}$$

By using QCD to extrapolate xF_3 to Q_0^2 however, one introduces α_s a priori into the result. Furthermore, higher twist effects are not included in QCD extrapolations,

In the new analysis, the CCFR data are combined with that of other neutrino experiments at low x and charged lepton scattering experiments at large x without Q^2 extrapolation at Q^2 values between 1 GeV^2 and 20 GeV^2 (see Fig.6). Evolving

the four lowest data points at $1 < Q^2 < 5$ GeV^2 to M_Z^2, the following value of α_s is obtained :

$$\alpha_s(M_Z^2) = 0.108 \pm^{0.003}_{0.005}(stat.) \pm 0.004\,(syst.) \pm^{0.004}_{0.006}(highertwist). \qquad (28)$$

This is a new competitive determination of α_s unfortunately limited by the badly known higher twist corrections.

3.4. *HERA experiments*

The first *determination* [41,42] of the proton structure function $F_2(x, Q^2)$ at HERA in 1992 has been based on a recorded luminosity of about 30 *rib-l* and has revealed the striking feature of a proton structure function rising as x decreases below 10^{-2}, for Q^2 values in the range $8 < Q^2 < 60$ GeV^2. The analysis of the 1993 data based on 10 to 20 times more integrated luminosity reported by the H1 43 and ZEUS 44 collaborations extends the kinematic range to a lower Q^2 value of 4.5 GeV^2 and to larger Q^2 values up to 2000 GeV^2. The 1994 data represents a further increase of about a factor 10 in statistics at large Q^2 together with an extension of the accessible kinematic range towards low Q^2 and very low x values. What limits the acceptance at low Q^2 can be easily seen from the following expression :

$$Q^2 = 4EE' \cos\frac{\theta^2}{2} \qquad (29)$$

where E is the energy of the incident electron and E' and θ are the energy and angle of the scattered electron relative to the incoming proton direction. In nominal running conditions the largest accessible angle is limited by the size of the beam pipe, The two HERA experiments have improved their detector closed to the beam pipe. In addition during a short dedicated run of the HERA collider of about 60 rib-l of recorded luminosity, the interaction point has been shifted by +65 cm in the proton beam direction [29,31], thus giving access to larger scattering angle (i.e. closer to the electron beam direction). The H1 collaboration has also used the events where the electron bunch collides with an early satellite proton bunch at about +65 cm of the nominal interaction point. An other method to increase the Q^2 acceptance is to select events where a photon of energy E_γ has been emitted collinear with the electron beam and detected about 90 m downstream in the electron direction. The measured $Q2$ value is then :

$$Q^2 = 4(E - E_\gamma)E' \cos(\frac{\theta^2}{2}) \qquad (30)$$

This method has allowed the H1 experiment 30 to reach $Q^2 = 1$ GeV^2.

With more statistics it has been also possible to carry on the tedious effort to decrease the systematic errors of the measurement of the structure function 17_2. The preliminary results of 1994 data have still systematic of about 10 % but there is

a reasonable hope to decrease the systematic down to 5 % in the final data. The normalisation errors in the large statistics 1994 H1 data sample taken with HERA nominal conditions has become almost negligible. It has been reduced to 1.5%

3.5. *Results*

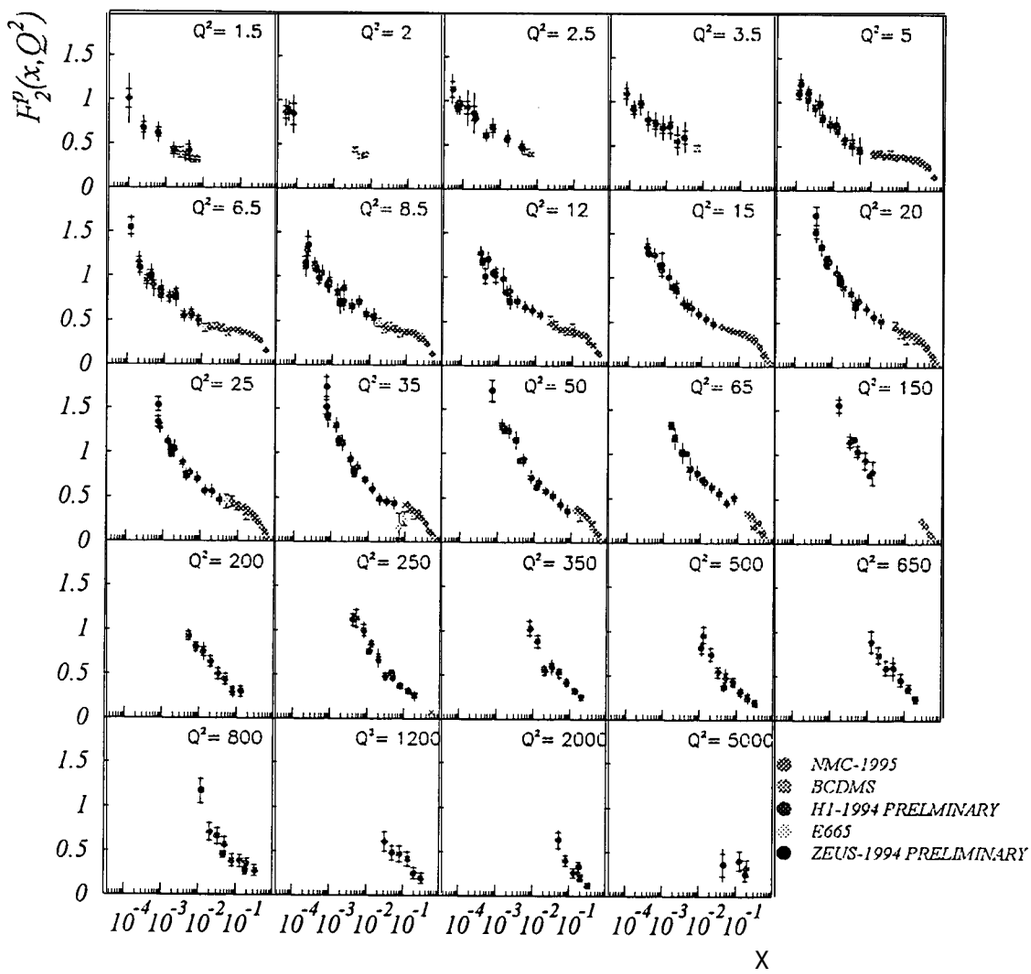

Fig. 7. Measurement of the proton structure function $F_2(x,Q^2)$ vs x for fixed values of Q^2. Preliminary 1994 data from H1 and ZEUS are compared to the fixed target data of BCDMS, E665 and NMC.

The results on $F_2(x,Q^2)$ from H1 and ZEUS together with those of BCDMS, E665 and NMC are shown in Fig. 7 as a function of x at fixed Q^2 values, The preliminary H1 data cover the full 1994 data set whereas the ZEUS data are so far restricted to

the low Q^2 shifted interaction point data and data points at very high Q^2. In all the bins where the comparison is possible the data sets of H1 and ZEUS agree well within the errors. There is also a smooth transition between the fixed target data and the HERA data. It is remarkable that the steep rise of F_2 with x decreasing persists to Q^2 values as low as 1.5 GeV^2 at $x < 10^{-2}$ and is already visible at $Q^2 = 2000$ GeV^2 at $x \sim 0.1$. At a fixed low x value, for example $x = 10^{-3}$, the steepness increases with Q^2 increasing.

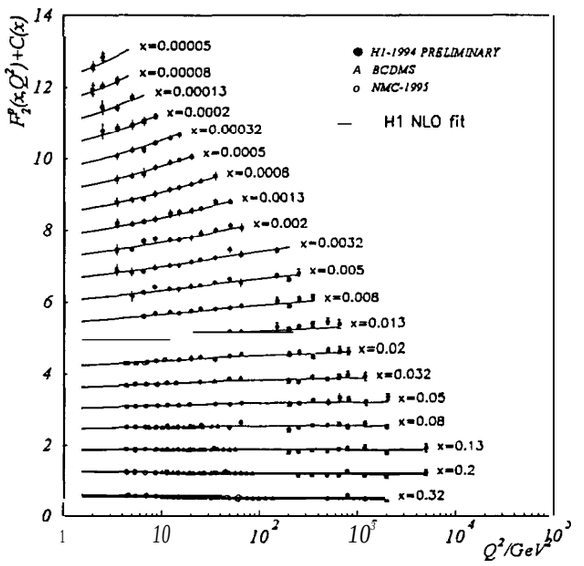

Fig. 8. Measurement of the proton structure function $F_2(x, Q^2)$ vs Q^2 for fixed values of x. Preliminary 1994 data from H1 (closed points) are compared to the fixed target data of BCDMS (open triangles) and NMC (open circles), The curves represent the DGLAP NLO QCD fit described in the text. For clarity the F_2 values are plotted, with all but normalisation errors, adding a term c(z) = $0.6(i_x - 0.5)$ to F_2, where i_x is the bin number starting at $i_x = 1$ for $x = 0.32$,

The H1 1994 data are also shown in Fig. 8 together with the data of BCDMS and NMC as a function of Q^2 at fixed x values. Here also the H1 data agree well with a smooth extrapolation from NMC and BCDMS data. As in the fixed target domain, there are no scaling violations at x $\sim$ 0.1, but pronounced Q^2 scaling violations at low x, steeper with x decreasing towards x = 0.00005.

4. QCD interpretation

The two salient features of the data at low x, rise of F_2 as x decreases and strong scaling violations, can be interpreted in perturbative QCD. The H1 collaboration has made a common fit of the 1994 preliminary data at $Q^2 > 5$ GeV^2 together with the new NMC data and the BCDMS measurements. The fit is based on Next-to-Leading Order (NLO) DGLAP evolution equations and it gives a very good description of

the data not only at $Q^2 > 5$ GeV^2 but also surprisingly down to $Q^2 = 1.5$ GeV^2 and $x = 0{,}00005$ (see Fig.8). Similar fits have been made on ZEUS or H1 1993 data combined with fixed target data [45,46,47,48]. All the fits require a starting distribution at $Q_0^2 = 4$ GeV^2 to be singular in $x^{-\lambda}$, with $\lambda \sim 0.2$ to 0.4, when x goes to zero. A value a bit smaller than in the bare pomeron of BFKL (equation 14). The fits give a satisfying description of the data, demonstrating that, within the present size of the errors, the DGLAP evolution equations are still valid in the HERA low x kinematic domain (see Fig.9). The fits have been used to determine the gluon density in the proton at very low x [49].

The H1 collaboration has also used the constraint at low x [48,9]. The quality of the fit is neither improved nor deteriorated.

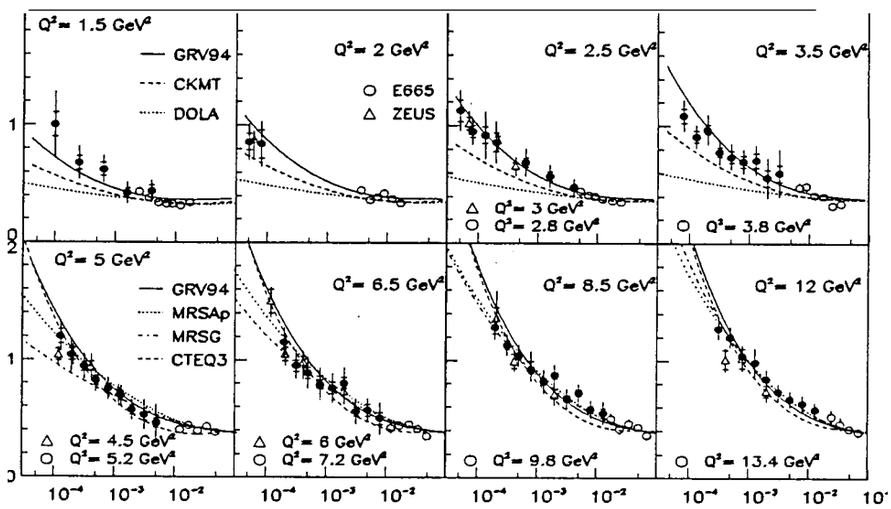

A quantitative way to test that perturbative QCD is the underlying dynamics of the rise at low x has been developed by Glück, Reya and Vogt (GRV)[50]. At a very low Q_0^2 = 0,34 GeV^2 value valence-like parton distributions are used as input to the DGLAP evolution equations. This yields a parametrisation of the structure function F_2 which is in accord with the data down to Q^2 = 1.5 GeV^2 (see Fig.9). It demonstrates that the DGLAP evolution equations are not only capable to describe the Q^2 evolution but also capable to generate the rise of F_2 with x decreasing provided a non singular input distribution is used at a very low Q^2 scale. This is in contrast to Regge inspired models [51,52] which are found not to describe the data even at the lowest Q^2 values at 1.5 GeV^2 (Fig.9).

4.2. Double scaling

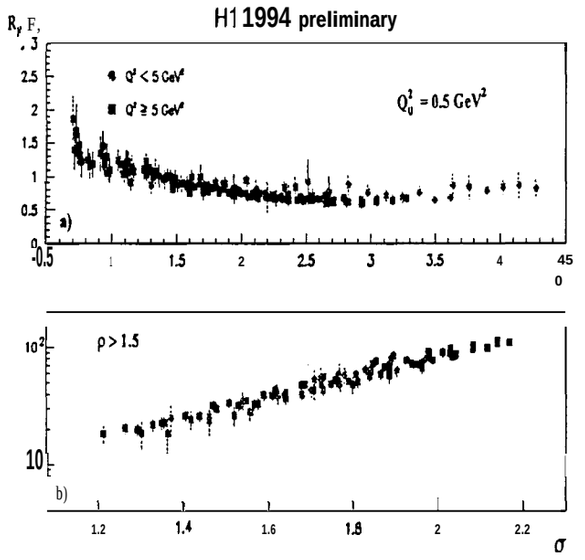

Figure 10: The rescaled structure functions $R'_F F_2$ and $\log(R_F F_2)$ plotted against σ and ρ where $\sigma = \sqrt{\log \frac{x_0}{x} \log \frac{t}{t_0}}$, $\rho = \sqrt{\log \frac{x_0}{x} / \log \frac{t}{t_0}}$ and $t_0 = \log Q_0^2/\Lambda^2$. The starting values are $x_0 = 0.1$ and $Q_0^2 = 0.5$ GeV^2. R_F and R'_F are simple rescaling factors to remove the trivial model-independent part of the prediction. The 1994 data points from H1 are preliminary.

To test the double scaling prediction, the H1 1994 data have been presented in Fig.10 in the variables σ and ρ where $\sigma = \sqrt{\log \frac{x_0}{x} \log \frac{t}{t_0}}$, $\rho = \sqrt{\log \frac{x_0}{x} / \log \frac{t}{t_0}}$ and $t_0 = \log Q_0^2/\Lambda^2$. More precisely it is the quantity $R_F F_2$ which is plotted, where R_F is

a trivial resealing factor :

$$R_F = \exp\left(-2\gamma\sigma + \frac{\delta\sigma}{\rho} + \frac{1}{2}\log\sigma + \log\rho\sigma\right) \tag{31}$$

and $\gamma = \sqrt{(12/\beta_0)}, \beta_0 = 11 - \frac{2}{3}n_f$ and $\delta = (11 + \frac{2}{27}n_f)/\beta_0$. In the double scaling limit $R_F F_2$ is predicted to be independent of both σ and ρ.

In Fig.10 we can see that provided the starting values are $x_0 = 0.1$ and $Q_0^2 = 0.5\,\mathrm{GeV}^2$ the scaling in ρ sets for $\rho \geq 1.5$ and that log $R'_F F_2 (= log\ R_F F_2 + 2\gamma\sigma)$ rises linearly with σ. The fact that HERA data agree well with the double scaling prediction is an other way to visualize, but without any fit, that perturbative QCD works well in the kinematic range explored so far at HERA. It is worth to stress that the variables σ and ρ are related to $\alpha_s(t)$. Double scaling is an evidence for the running of $\alpha_s(Q^2)$[53].

4.3. α_s *from low x data*

It is well known that one of the most precise determinations of α_s comes from the analysis of the Q^2-scaling violations of structure functions in the fixed target kinematic domain 4. Because the HERA data at low z seem to be free of non perturbative uncertainty, Ball and Forte [53] have extracted α_s from the low x 1993 HERA data H1 and ZEUS. The method uses NLO evolution equations in various renormalization schemes and based either on the usual summation of leading $(\alpha_s \log Q^2)^n$ terms, as in DGLAP equations, or on NLO summations of leading $(\alpha_s \log Q^2 \log \frac{1}{x})^n$ as should naively be more appropriate at low x. They conclude that the data are not yet sufficient to show to what extent a special summation is necessary. In the two types of approach, HERA data are very sensitive to α_s. The quoted value is

$$\alpha_s(M_Z) = 0.120 \pm 0.005(exp) \pm 0.009(th.). \tag{32}$$

The theoretical error is dominated by the renormalization and factorization scheme ambiguities.

4.4. *Summary on interpretations*

We have seen that the HERA data can be equally described by either usual NLO fits with a singular starting distribution at $Q_0^2 = 4\ \mathrm{GeV}^2$ or by the GRV parametrisation with a non singular starting distribution at $Q_0^2 = 0.34\ \mathrm{GeV}^2$. We have also seen that the double scaling sets up at small value of ρ.

extracted. The data do not yet require to restrict the summation to large $(\alpha_s \log(\frac{1}{x}))^n$ terms, as in BFKL equation, and not even to the $(\alpha_s \log \frac{1}{x} \log Q^2)^n$ terms. It is however anticipated that less inclusive measurements of the hadronic final state, as the gluon emission in the hadronic cascade (Fig. 2) which accompany the scattered electron, would be more sensitive to the mechanism of summation that the structure functions [9].

5. Future prospects

After the final publications of all fixed target data and the rejuvenation brought by HERA to the field of structure functions there is still a high statistics high precision neutrino scattering experiment scheduled to start in 1996, the Fermilab E815 experiment (NuTeV) and at HERA there is more than one order of magnitude of luminosity which can be gained. The next experimental challenges will be

- to improv. significantly the precision of the measurement at $Q^2 > 1.5$ GeV^2 in order to decrease the error on α_s and eventually reveal the underlying dynamics at low x,
- to extent the kinematical range down to $Q^2 \sim 0.1$ GeV^2 to understand the transition to the non perturbative domain of photoproduction and to study the limits of perturbative approach à la GRV,
- to get precise measurements at high $Q^2 (Q^2 > 1000$ GeV$^2)$ where HERA physics has hardly started [54,55], eventually the most attractive part would be deviations from the standard model.

In conclusion, there is no doubt that measurement of structure functions and more generally of lepton-nucleon scattering is again a very active field which will bring in the next future more insight into our knowlege of interactions and matter.

6. Acknowledgements

It is a pleasure to thank Dusan Bruncko, Ladislav Sandor and Jozef Urban together with the charming crew of Kosice to have organised a so exciting symposium in the beautiful High Tatra Mountains. Many thanks also to my H1 colleagues Albert De Roeck, Ralph Eichler, Jean-Francois Laporte, Gaby Raedel and Christopher Royon for help in preparing the manuscript.

1. H. Georgi and H.D. Politzer, *Phys. Rev.* **D9** (1974) 416,
2. D.J. Gross and F. Wilczek, *Phys. Rev.* **D9** (1974) 980.
3. V.N. Gribov and L.N. Lipatov, *Sov. J. Nucl. Phys.* **15 (1972) 438** and 675; G. Altarelli and G. Parisi, *Nucl. Phys.* **B126** *(1977)* 298 ; Yu.L. Dokshitzer, *Sov. Phys. JETP 46 (1977) 641.*

4. M. Virchaux, *QCD* **20** *years later, Proceedings of Aachen conf.*, eds P.M. Zerwas and H.A. Kastrup (World Scientific, 1993) page 205.
5. E.A. Kuraev, L.N. Lipatov and V.S. Fadin, *Phys.Lett.* **B60** (1975) 50 ; Ya.Ya. Balitski and L.N. Lipatov, *Sov. J, Nucl. Phys. 28 (1978) 822* and *Zh. Eksperiment. I. Teor.Fiz. 72 (1977) 377.*
6. M. Ciafaloni,
7.
8.
9.

28, E-665 FNAL Collaboration, A. Kotwal, preprint **FERMILAB-CONF-95-046-E** and proceedings of the *XXXth Rencontres de Moriond*, 19-25 Mars 1995.
29. H1 Collaboration, **EPS-0470** and U. Strauman, proceedings of the *EPS-HEP95 Conference,* Brussels, 1995.
30. H1 Collaboration, **EPS-0472** and U. Strauman, proceedings of the *EPS-HEP95 Conference,* Brussels, 1995.
31. ZEUS Collaboration, **EPS-0392** and F.Chlebana, proceedings of the *EPS-HEP95 Conference,* Brussels, 1995 and preprint **DESY** 95-193; A. Caldwell proceedings of *XVII International Symposium on Lepton Photon Interactions,* Beijing, China, August 1995.
32. BCDMS Collaboration, A.C.Benvenuti et al., *Phys.Lett.* **B223** *(1989) 485.*
33. L.W.Whitlow et al., *Phys.Lett.* bf B282 (1992) 475.
34. CCFR Collaboration, D.A. Harris et al., proceedings of the *Workshop on Deep Inelastic Scattering and QCD*, Paris, April 1995.
35. NMC Collaboration, P. Amaudruz et al., *Phys.Lett.* **B295** *(1992) 159.*
36. NMC Collaboration, M. Arneodo et al., *Phys. Rev. 50 (1994)* R1.
37. NMC Collaboration, M. Arneodo et al., *Phys. Rev. Lett. 66 (1991) 2712.*
38. A.D. Martin, W.J. Stirling, R.G. Roberts, *Phys.Lett.* **B252** *(1990) 653.*
39. W. Wittek, these proceedings.
40. CCFR Collaboration, W.C.Leung et al., . *Phys.Lett.* **B317** *(1993) 655,*
41. H1 Collaboration, I. Abt et al., it Nucl.Phys. **B407** (1993) 515.
42. ZEUS Collaboration, M. Derrick et al. *Nucl.Phys.* **B316** *(1993) 412.*
43. H1 Collaboration, T. Ahmed et al., *Nucl.Phys.* **B439** *(1995) 471.*
44. ZEUS Collaboration, M. Derrick et al., *Z.Phys.* **C65** *(1995) 379.*
45. A.D. Martin, R.G. Roberts and W.J.Strirling, preprint **RAL** 95-021 (1995)
46. CTEQ Collaboration, H.L.Lai et al. *Phys. Rev.* **D51** *(1995) 4763.*
47. ZEUS Collaboration, M. Derrick et al., *Phys.Lett.* **B345** *(1995) 576.*
48. H1 Collaboration, S. Aid et al., *Phys.Lett.* **B354** *(1995) 494.*
49. M. Botje, these proceedings.
50. M. Glück, E. Reya and A. Vogt, preprint **DESY** 94-206 (1994).
51. A. Donnachie and P.V.Landshoff, Z. *Phys.* **C61** *(1994) 139.*
52. A. Capella et al., *Phys.Lett.* **B337** *358.*
53. R.D. Ball and S. Forte, *Phys.Lett.* **B358** *(1995) 365.*
54. H1 Collaboration, S. Aid et al., *Phys.Lett.* **B353** *(1995) 578.* and *Z.Phys.* **C67 (1995) 565**; paper **EPS-0466** submitted to the *EPS-HEP95 Conference,* Brussels, 1995.
55. ZEUS Collaboration, M. Derrick et al., preprint **DESY** 95-053.